

This article was downloaded by: [University of California, San Diego]

On: 07 August 2012, At: 12:20

Publisher: Taylor & Francis

Informa Ltd Registered in England and Wales Registered Number: 1072954 Registered office: Mortimer House, 37-41 Mortimer Street, London W1T 3JH, UK



## Molecular Crystals and Liquid Crystals

Publication details, including instructions for authors and subscription information:

<http://www.tandfonline.com/loi/gmcl20>

### Frederiks Transition in the Nematic and Smectic A Phases of Polar Thioesters

J. Chruściel<sup>a</sup>, J. Czerwiec<sup>b</sup>, M. Jaglarz<sup>b</sup>, M. Marzec<sup>b</sup>, A. Wawrzyniak<sup>b</sup>, M. D. Ossowska-Chruściel<sup>a</sup> & S. Wróbel<sup>b</sup>

<sup>a</sup> Institute of Chemistry, Siedlce University of Natural Sciences and Humanities, Siedlce, Poland

<sup>b</sup> Institute of Physics, Jagiellonian University, Kraków, Reymonta, Poland

Version of record first published: 16 Jun 2011

To cite this article: J. Chruściel, J. Czerwiec, M. Jaglarz, M. Marzec, A. Wawrzyniak, M. D. Ossowska-Chruściel & S. Wróbel (2011): Frederiks Transition in the Nematic and Smectic A Phases of Polar Thioesters, *Molecular Crystals and Liquid Crystals*, 547:1, 268/[1958]-275/[1965]

To link to this article: <http://dx.doi.org/10.1080/15421406.2011.572782>

PLEASE SCROLL DOWN FOR ARTICLE

Full terms and conditions of use: <http://www.tandfonline.com/page/terms-and-conditions>

This article may be used for research, teaching, and private study purposes. Any substantial or systematic reproduction, redistribution, reselling, loan, sub-licensing, systematic supply, or distribution in any form to anyone is expressly forbidden.

The publisher does not give any warranty express or implied or make any representation that the contents will be complete or accurate or up to date. The accuracy of any instructions, formulae, and drug doses should be independently verified with primary sources. The publisher shall not be liable for any loss, actions, claims, proceedings, demand, or costs or damages whatsoever or howsoever caused arising directly or indirectly in connection with or arising out of the use of this material.

## Frederiks Transition in the Nematic and Smectic A Phases of Polar Thioesters

J. CHRUŚCIEL,<sup>1</sup> J. CZERWIEC,<sup>2</sup> M. JAGLARZ,<sup>2</sup>  
M. MARZEC,<sup>2</sup> A. WAWRZYNIAK,<sup>2</sup>  
M. D. OSSOWSKA-CHRUŚCIEL,<sup>1</sup> AND S. WRÓBEL<sup>2</sup>

<sup>1</sup>Institute of Chemistry, Siedlce University of Natural Sciences and Humanities, Siedlce, Poland

<sup>2</sup>Institute of Physics, Jagiellonian University, Kraków, Reymonta, Poland

*Dielectric and electro-optic properties of two homologues of 4-chlorophenyl 4'-n-alkoxythiobenzoates, showing nematic and smectic A phases with positive dielectric anisotropy, were studied. Planar alignment of the nematic was obtained upon slowly cooling from the isotropic phase using ITO planar cell. Upon further slowly cooling to the smectic phase one can obtain its planar texture. Reversible Frederiks transition was observed for nematic phase in AC field. It is possible to measure the splay elastic constant which changes discontinuously at the nematic-smectic A transition. However, in the smectic phase Frederiks transition was irreversible and the threshold voltage was much higher.*

**Keywords** Conductivity anisotropy; dielectric anisotropy; Frederiks transition; planar and homeotropic texture; splay elastic constant; threshold voltage

### 1. Introduction

Theoretically for highly polar compounds – composed of molecules with permanent dipole moments being parallel to the long molecular axes – a rich polymorphism of the SmA phase occurs [1]. For the compounds studied the SmA<sub>2</sub> phase shows up most probably (Fig. 1(b)).

Highly polar thioesters with nitro group at para position displaying only SmA phase which exhibits irreversible Fredericks transition was studied by us before [2]. New asymmetric thioesters with chlorine atom at para position show N and smectic A polymorphism [3]. They exhibit positive and strong dielectric anisotropy which facilitates Frederiks transition. In this study two principal electric permittivities and conductivities were measured vs. temperature. The elastic constant  $k_{11}$  was computed based on dielectric and electro-optic data.

---

Address correspondence to S. Wróbel, Institute of Physics, Jagiellonian University, 30-059 Kraków, Reymonta, Poland. Tel.: +48-12663 5684; Fax: +48-126337086; E-mail: stanislaw.wrobel@uj.edu.pl

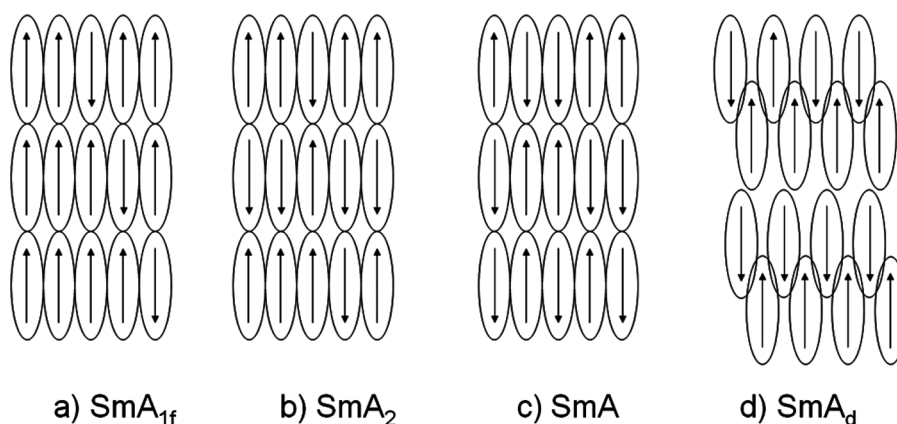


**Figure 1.** Models of SmA for liquid crystalline compounds having large permanent dipole moments along the long molecular axis [1]. a) Ferroelectric like order – positive dipole-dipole correlation, b) Double-layer SmA phase with negative dipole-dipole correlation, c) Normal SmA phase, d) Interdigitated  $\text{SmA}_d$  phase – strongly correlated double layers due to overlapping of molecules in neighboring layers.

We have found out that the last point could be an interesting experiment for student's laboratory as it bears the following advantages: 1. Students can learn how a mono-domain texture can be grown; 2. One can demonstrate that Frederiks transition is reversible in nematic phases what is very important for display application. On the other hand in SmA phase this transition is irreversible; 3. Students can learn that for the smectic A phase both quantities the threshold voltage and the  $k_{11}$  splay elastic constant are much larger than those for the nematic phase; and 4. The character of the nematic-smectic A phase transition can be also studied.

## 2. Experimental

### 2.1. Synthesis

We present a convenient synthesis of mesogens containing two phenyl rings and COS central bonding, belonging to new homologous series of thiobenzoates, 4-chlorophenyl 4'-n-alkoxythiobenzoates,  $\text{C}_n\text{H}_{2n+1}\text{O-Ph-COS-Ph-Cl}$ , which we refer to as nOSCl (n denotes the number of carbon atoms in the alkoxy chain), in which the chlorine is *p*-substituted in the phenyl ring.

The nOSCl compounds were synthesized according to the route shown in Figure 2. The 4-n-alkoxybenzoic acid  $\text{C}_n\text{H}_{2n+1}\text{O-C}_6\text{H}_4\text{COOH}$ , (nOB (1)) were used as the starting compounds for the synthesis of the 4-n-chlorophenyl 4-n-alkoxythiobenzoates (nOSCl (2)). Alkoxybenzoyl chlorides, the intermediates for the synthesis

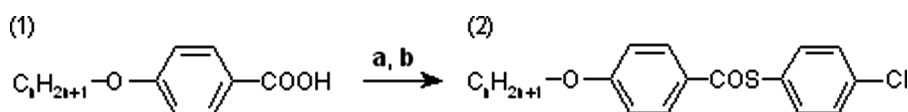


**Figure 2.** Synthesis of nOSCl [a:  $\text{SOCl}_2$ , toluene; b:  $\text{HSC}_6\text{H}_4\text{Cl}$ ,  $(\text{C}_2\text{H}_5)_3\text{N}$ ].

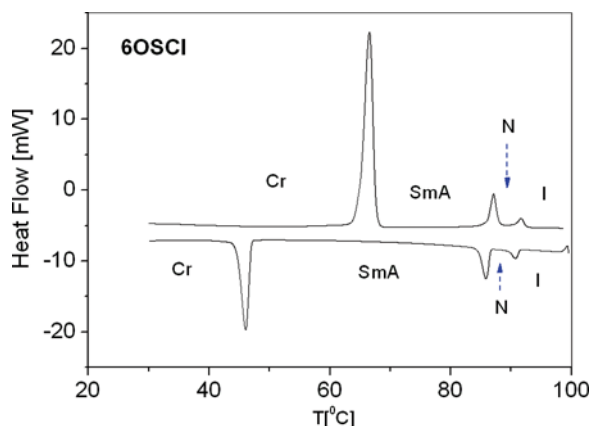


**Figure 3.** DSC thermograms obtained for 6OSCl. (Figure appears in color online.)

of nOSCl, were obtained by reaction of the 4-n-alkoxybenzoic acid and thionyl chloride in anhydrous toluene. The final liquid crystal compounds (2) were purified by recrystallization from ethanol, giving 80–90% yields and using gel column chromatography. The synthesis was described in detail in [4].

The structure of the nOSCl compounds were confirmed by NMR, IR, mass and elemental analysis. The NMR spectra were obtained using an NMR Varian 500 spectrometer ( $\text{CDCl}_3$ , TMS as internal standard), IR spectra were recorded by an FTIR Nicolet Magna 760 spectrometer and a minimum of 64 co-added scans at the resolution of  $1\text{ cm}^{-1}$ . The mass spectrum were obtained using a TOF MS  $\text{ES}^+$  spectrometer. Transition temperatures were determined by complementary methods: polarizing optical microscopy (POM), transmittance light intensity (TLI) [5] and the enthalpy and entropy changes were determined by differential scanning calorimetry (DSC).

## 2.2. DSC Calorimetry

Phase transitions were studied by means of DSC calorimetry using Perkin-Elmer DSC8000. As found using both DSC thermograms (Fig. 3) and texture observation (Figs. 4 (a)–(d)) both materials studied possess nematic and smectic A phases.

## 2.3. Texture Observation

5OSCl and 6OSCl were very well aligned in planar cells giving a uniform texture. Since both materials exhibit positive dielectric anisotropy a reversible transition between planar and homeotropic textures have been observed for nematic phases (Figs. 4 (a) and (b)). In the case of smectic phase an irreversible planar-homeotropic transition has been observed (Figs. 4(c) and (d)).

## 2.4. Dielectric Spectroscopy

The principal components of the dielectric permittivity tensor (Eq. (1)) were measured by using the dielectric spectrometer based on Agilent 4294A impedance

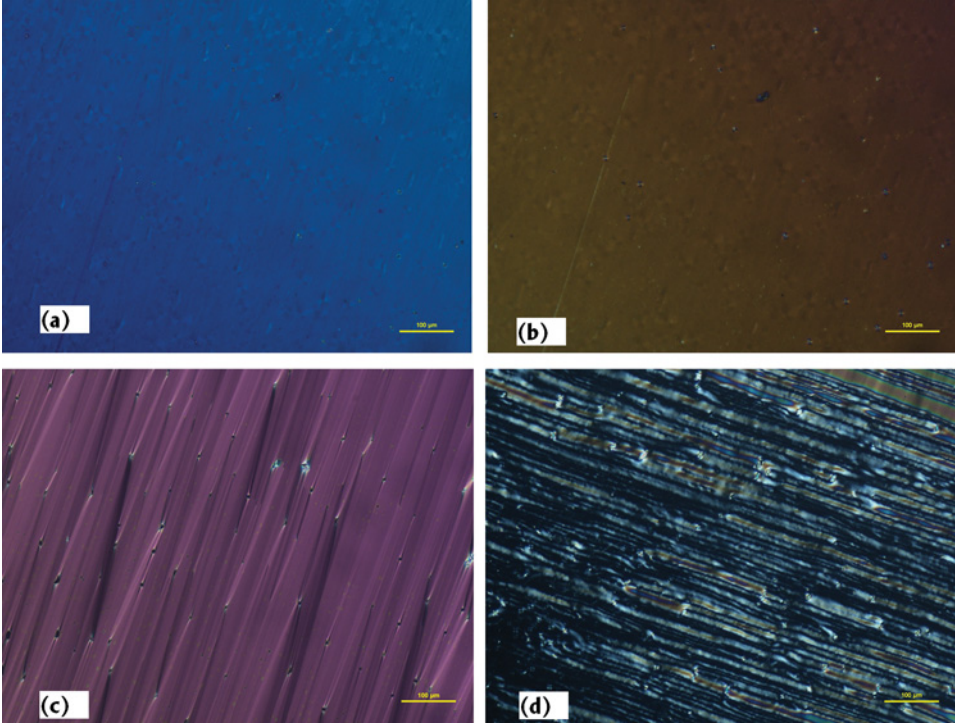


**Figure 4.** (a) Planar and (b) homeotropic (at  $8 V_{p-p}$ ) texture of N phase of 6OSCl at  $85^\circ\text{C}$  (c) Planar and (d) homeotropic (at  $110 V_{p-p}$ ) texture of SmA of 6OSCl phase at  $79^\circ\text{C}$ . (Figure appears in color online.)

analyzer.

$$\hat{\varepsilon} = \begin{Bmatrix} \varepsilon_{\perp} & 0 & 0 \\ 0 & \varepsilon_{\perp} & 0 \\ 0 & 0 & \varepsilon_{\parallel} \end{Bmatrix}, \quad (1)$$

where  $\varepsilon_{\perp}$  is measured for planar texture, and  $\varepsilon_{\parallel}$  - for homeotropic alignment. Both principal conductivities ( $\sigma_{\perp}$  and  $\sigma_{\parallel}$ ) have also been measured. One should apply very weak measuring electric field. Two kinds of special AWAT  $5 \mu\text{m}$  - cell with gold electrodes were used - one cell for planar and the other one for homeotropic alignment. The planar HG cell had gold electrodes with rubbed polymer layers, whereas the homeotropic HT cell had electrodes covered with surfactant giving homeotropic alignment. In dielectric measurements cells without surface treatment to obtain proper values of the dielectric and conductivity anisotropies were also used. Homeotropic and planar textures of the SmA phase obtained by slowly cooling from the nematic phase are shown Figure 4.

For homeotropic alignment a strong dielectric relaxation process (Figs. 5 (a) and (b)) was found with large activation energy characteristic for the reorientation of molecule around the short molecular axis.

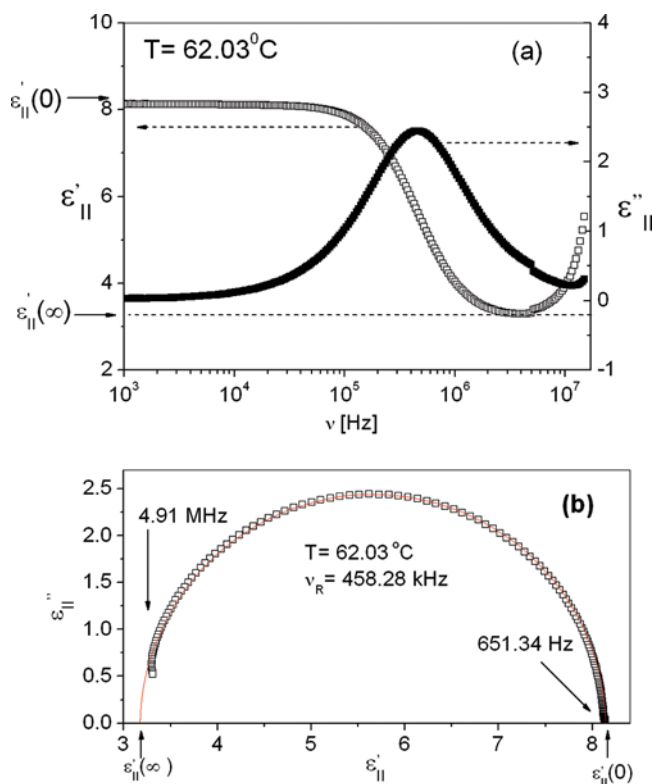


**Figure 5.** (a) Dielectric spectrum for SmA phase of 6OSCl, (b) Cole-Cole diagram for SmA phase of 6OSCl. (Figure appears in color online.)

This dielectric relaxation process can be described by the Debye model with conductivity term:

$$\epsilon^*(\omega) = \epsilon'(\omega) - i\epsilon''(\omega) = \epsilon(\infty) + \frac{\Delta\epsilon_S}{1 + (i\omega\tau)^{1-\alpha}} - i\frac{\sigma(\omega)}{\epsilon_0\omega}, \quad (2)$$

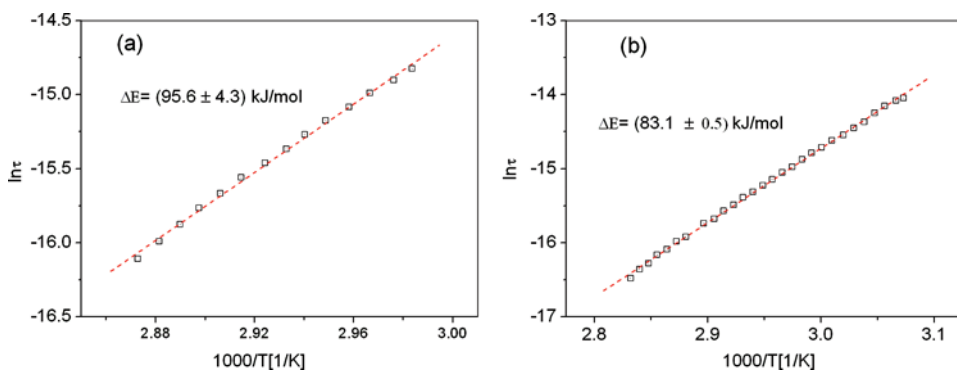


**Figure 6.** Arrhenius plots the relaxation process originated from molecular reorientation around the short axis – (a) 5OSCl, (b) 6OSCl. (Figure appears in color online.)

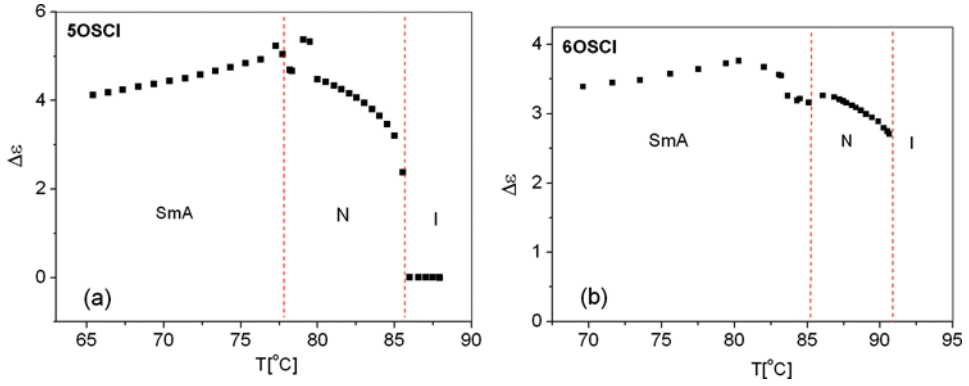


**Figure 7.** (a) Dielectric anisotropy of 5OSCI, (b) Dielectric anisotropy of 6OSCI. (Figure appears in color online.)

where:  $\epsilon(\infty)$  is the high frequency limit of electric permittivity,  $\Delta\epsilon_s$  is the dielectric increment of the relaxation process related to reorientation around the short molecular axis,  $\epsilon_o$  is electric permittivity of free space,  $\tau$  is the relaxation time,  $\alpha$ -distribution parameter,  $\sigma$ -ionic conductivity,  $\omega = 2\pi\nu$  is a circular frequency of measuring field. By fitting Eq. (2) to the experimental points one can find that the Debye model (with  $\alpha = 0.0$ ) describes very well the relaxation process studied for homeotropic alignment of the SmA phase for both materials. The values of activation energies (Figs. 6(a) and (b)) indicate that one has to do here with molecular reorientation around the short axis.

## 2.5. Electro-Optic Experiment

The threshold voltage was measured using an electro-optic set-up which consists of polarizing microscope with INSTEC temperature controller. The transmission of light can be measured by digital camera or recorded by a photodiode. The HG planar electro-optic cell is heated above the clearing point of the material studied. A small amount of degassed liquid crystal (in form of a button) is being put against the capillary gap of the HG cell. One in the isotropic phase the material fills out the cell. Upon slowly cooling one can grow a homogenous planar nematic mono-domain (Fig. 4(a)) which upon further cooling transforms into planar smectic A phase (Fig. 4(c)).

Such planar mono-domain can be switched from planar to homeotropic alignment when one applies an electric field equal to the threshold voltage ( $V_{th}$ ) or higher. The following equation allows computing the  $k_{11}$  splay elastic constant:

$$k_{11} = \frac{U_{th}^2 \epsilon_o \Delta\epsilon}{\pi^2}, \quad (3)$$

where:  $\epsilon_o$  is electric permittivity of free space,  $\Delta\epsilon = \epsilon_{||}(0) - \epsilon_{\perp}(0)$  is the dielectric anisotropy.

## 3. Results and Discussion

### 3.1. Dielectric Anisotropy

Dielectric anisotropy behaviour with temperature shows that at low temperatures formation of double layer structures of the smectic A phase (Fig. 1(b)) takes place

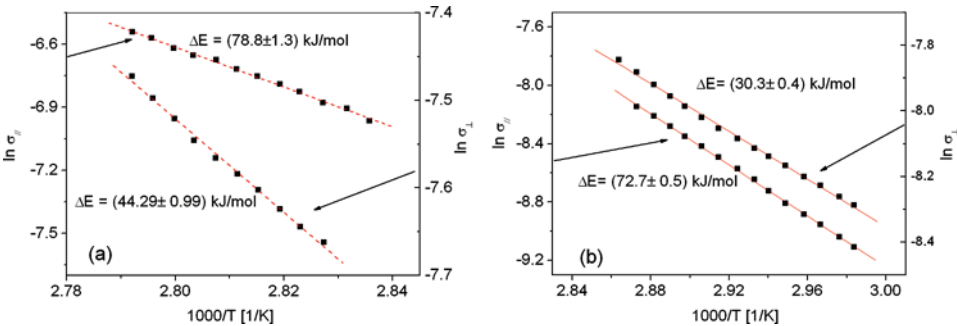


**Figure 8.** (a) Activation energy for principal conductivities for N phase of 5OSCI, (b) Activation energy for principal conductivities for SmA<sub>2</sub> phase of 5OSCI. (Figure appears in color online.)

as predicted by the theory [1]. Greater stability of the smectic double layers in the low temperature range of the SmA phase causes bigger conductivity anisotropy (Fig. 8(b)) and larger  $k_{11}$  elastic constant which saturates at low temperatures (Figs. 9(a) and (b)).

Dielectric studies show that both compounds exhibit negative dipole – dipole correlation in their SmA phases. As seen in Figures 7(a) and (b) the dielectric anisotropy  $\Delta\epsilon$  decreases with decreasing temperature.

### 3.2. Conductivity Anisotropy

As found the conductivity anisotropy is negative in the SmA phase (Figs. 8(a) and (b)) whereas for the nematic phase it is positive. It is interesting that for both phases diffusion of ions perpendicular to the director has much smaller activation energy (by factor 2) than parallel to the director.

The dielectric measurements show that the dielectric anisotropy (Figs. 6 (a) and (b)) in the nematic phase fulfils Maier-Meier theory whereas in the smectic A phase negative dipole-dipole correlation leads to its decreasing. It may be a sign of bi-layer formation characteristic for SmA<sub>2</sub>.

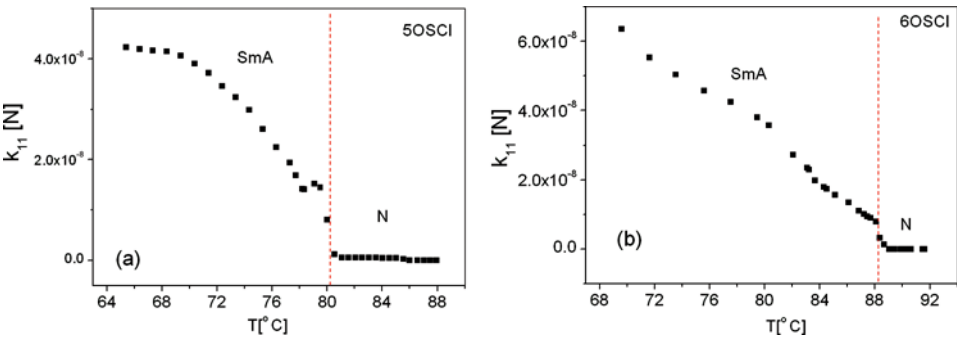


**Figure 9.** Elastic constant vs. temperature – (a) 5OSCI and (b) 6OSCI. (Figure appears in color online.)



### 3.3. Elastic Constant

Dielectric and electro-optic studies allowed us to compute the splay elastic constant ( $k_{11}$ ) for the nematic and SmA phases of both compounds. As found  $k_{11}$  is for the SmA phase (Figs. 9(a) and (b)) three orders of magnitude higher than for nematics what is caused by greater stability of bilayer structure due to dipole-dipole interaction. Frederiks transition for the nematic phase is reversible whereas for the SmA – irreversible.

As seen the elastic constant changes discontinuously at the nematic-smectic A transition.

## 4. Conclusions and Perspectives

As found  $k_{11}$  is three orders of magnitude higher for the SmA phase than for nematics what is caused by greater stability of bilayer structure due to dipole-dipole interaction. Frederiks transition for the nematic phase is reversible whereas for the SmA – irreversible.

The conductivity anisotropy ( $\Delta\sigma$ ) of both substances changes its sign at the nematic-SmA transition from positive to negative which means that migration of ions is easier within than across the layers.

The values of activation energy obtained for the substances studied on the basis of temperature dependence of conductivity confirm the idea that the diffusion of particles inside the layers is much easier than between the layers. The activation energy for the former process is by factor 2 smaller.

## Acknowledgment

Financial support of the State Committee for Scientific Research (KBN) under the grant No. N N202 076435 is gratefully acknowledged.

The research was carried out with the equipment purchased thanks to the financial support of the European Regional Development Fund in the framework of the Polish Innovation Economy Operational Program (contract no. POIG.02.01.00-12-023/08).

## References

- [1] Longa, L., Trebin, H.-R., & Cholewiak, G. (2003). Computer simulations of polar liquid crystals. In: *Relaxation Phenomena*, Haase, W., & Wróbel, S. (Eds.), Springer-Verlag: Heidelberg.
- [2] Ossowska-Chruściel, M. D., Mikułko, A., Karkuszevska, I., Wróbel, S., Chruściel, J., Marzec, M., & Haase, W. (2005). Frederiks transition in smectic A Phase of a strongly polar tioester. In: *Neutron Scattering and Complementary Methods in Investigations of Condensed Phase*, Chruściel, J., Szytuła, A., & Zajac, W. (Eds.), Univ. of Podlasie Publishing House: Siedlce.
- [3] Mikułko, A., Fraś, M., Marzec, M., Wróbel, S., Ossowska-Chruściel, M. D., & Chruściel, J. (2008). *Acta Phys. Polonica*, 113, 1155.
- [4] Ossowska-Chruściel, M. D., Roszkowski, P., Rudzki, A., & Chruściel, J. (2005). *Liq. Cryst.*, 32, 877.
- [5] Ossowska-Chruściel, M. D., Zalewski, S., Rudzki, A., Feliks, A., & Chruściel, J. (2006). *Phase Transit.*, 79, 679.
- [6] Bunning, J. D., Faber, T. E., Sherell, P. L., et al. (1981). *J. de Physique*, 42, 1175.